Journal of Ceramic Processing Research. Vol. 24, No. 5, pp. 850~859 (2023)
(Received 21 July 2023, Received in revised form 30 September 2023, Accepted 1 October 2023)
https://doi.org/10.36410/jcpr.2023.24.5.850

J O U R N A L O F
Ceramic Processing Research

Unleashing the resilience of Reinforced Concrete Member retrofitted with composite laminates

K.S. Navaneethan[a,*], S. Anandakumar[b], S. Manoj[c] and P.C. Murugan[d]
[a]*Department of Civil Engineering, Kongu Engineering College, Perundurai, Erode, Tamil Nadu - 638060, India*
[b]*Department of Civil Engineering, KPR Institute of Engineering and Technology, Coimbatore, Tamil Nadu - 641407, India*
[c]*Department of Civil Engineering, Kongu Engineering College, Perundurai, Erode, Tamil Nadu - 638060, India*
[d]*Department of Automobile Engineering, Kongu Engineering College, Perundurai, Erode - 638060, India*

This work presents experimental results on the performance of Aramid Fiber Reinforced Polymer (AFRP) laminates used in the flexural retrofitting of full-scale reinforced concrete beams. The effects of variables including reinforcement placement, retrofitting orientation, and AFRP lifespan are examined. The experimental findings provide compelling evidence that structurally damaged beams can be retrofitted with AFRP composite material to restore their strength and stiffness. In most cases, the retrofitted beams perform as well as, if not better than, the control beams. The efficiency of the AFRP strengthening method in flexure, however, was found to vary with beam length. The examinations revealed that plate debonding was the leading cause of the failures observed. In order to overcome this difficulty, it is crucial to enhance the bonding processes between the AFRP laminates and the concrete substrate.

Keywords: Aramid Fibre Reinforced Polymer (AFRP), Retrofitting, Laminate, Rupture of reinforced concrete beam, Debonding.

Introduction

There are already a lot of buildings that don't meet the structural requirements. This could be because the design standards were changed, the load was increased, the reinforcement bars rusted, or there was a mistake during construction or an accident, like an earthquake [1]. To address inadequate capacity, structures must be updated or renovated. There are various types of strength enhancing materials available on the market [2-4]. Ferro-cement strengthening, steel plate jacketing, and polymer laminates reinforced with fibers are all examples of these [5-7]. The service and ultimate load capacities of existing concrete elements can be greatly improved with the retrofitting of RC elements by strengthening with fiber-reinforced polymer (FRP) plates or sheets [8-10]. It is better for the environment and the economy to restore or strengthen structures instead of building new ones. With the emergence of structurally sound adhesives, the use of FRP composite materials to strengthen things has gone up by a broad range. FRP is becoming more popular than steel plates due to its lightweight, high rigidity and strength-to-weight ratio [11-13], resistance to corrosion, reduced maintenance costs, and faster installation time. The addition of Aramid fibre-reinforced polymer (AFRP) laminate over the surface of reinforced concrete beams can make the beams more rigid and able to support more loads, according to past research.

The moment capacity of aged concrete beams has been improved by the addition of a CFRP or GFRP externally bonded composite [3, 4, 14-16]. Despite the abundance of research on the performance of retrofitted beams, the impact of CFRP length on the performance of pre-cracked there is a lack of research on the flexure and shear behavior of preloaded concrete beams with CFRP retrofits. In this experimental investigation, the effects of incorporating AFRP laminates into the construction of RC-beams were investigated.

Aramid fiber reinforced plastic (AFRP) is a suitable material for enhancing the strength of retrofitting beams by up to 120%, minimizing deflections, and improving stiffness by up to 105% due to its high strength-to-weight ratio. AFRP has a number of advantages, some of which include enhanced load-carrying capacity, durability, and the simplicity of installation on concrete surfaces with no structural damage [20]. AFRP also has a longer service life. To ensure this was feasible, full-scale beams have been evaluated in the lab. The length of the AFRP and the ratio of reinforcing steel play pivotal roles in this analysis.

Material and techniques

Fifteen Reinforced concrete beams with minimal

*Corresponding author:
Tel : +91 8056554879
E-mail: navaneethan.kec@gmail.com

Table 1. Mechanical Characteristics of Polymer Composites Reinforced with Aramid Fibers.

Composite material	Yield force (N)	Yield elongation (mm)	Break force (N)	Flexural at yield (N/mm^2)	Flexural strength at break (N/mm^2)	Impact load (Joule)
Aramid Fiber reinforced polymer composites	392.28	4.87	843.4	24.57	29.195	0.552

support were subjected to a set of four-point bending tests for this investigation. In addition, tests were run on the concrete, reinforcing steel, and AFRP used to build the beams to determine their mechanical qualities. Concrete of moderate durability was produced using a blend of water, gravel, and Regular Portland cement. Coarse, crushed limestone and silica sand were used as the aggregate material. A slump of 50 mm and a compressive strength of 20 MPa at 28 days were targeted for the concrete blend. The ratio of free water to cement was 0.45 [17, 18], and the maximum aggregate size was 20 mm. Concrete is a construction material that possesses notable properties such as high compressive strength and splitting tensile strength. It exhibits an elastic modulus of 23.7 GPa and a compressive strength of 24.58 MPa. Additionally, it has a splitting tensile strength of 2.146 MPa. Steel, on the other hand, is commonly used for its exceptional tensile strength. The two steel grades mentioned, D6 and D8, have different properties. The D6 steel has an elastic modulus of 204.0 GPa, a yield stress of 425.16 MPa, and an ultimate stress of 435.30 MPa. The D8 steel, on the other hand, possesses an elastic modulus of 226.2 GPa, a yield stress of 425.16 MPa, and an ultimate stress of 435.30 MPa.

The above Table 1 provides mechanical properties of Aramid Fiber Reinforced Polymer (AFRP) composites. The yield force represents the amount of force required to cause a permanent deformation or change in shape of the material. In this case, the AFRP composites have a yield force of 392.28 N. Yield elongation refers to the amount of elongation or stretching the material undergoes before reaching its yield point. The yield nature of the AFRP laminates were studied with sem analysis. The AFRP composites exhibit a yield elongation of 4.87 mm.

The above Fig. 1 shows the SEM images of AFRP laminates reveal the distribution and orientation of aramid fibers as part of the polymer matrix, revealing important details about the reinforcement's efficacy. It was found that spherical Aramid Fiber-Reinforced Polymer (AFRP) composites had better fluidity and higher visual density than their standard AFRP peers. Because of the faster metallurgical process, different AFRP-reinforced phases were formed on-site, which led to this improvement. Micrographs can show how well aramid fibers are bonded to a polymer matrix. For effective load transmission and enhanced mechanical qualities, a well-bonded contact with strong adhesion is preferred. The incorporation of specific phases within

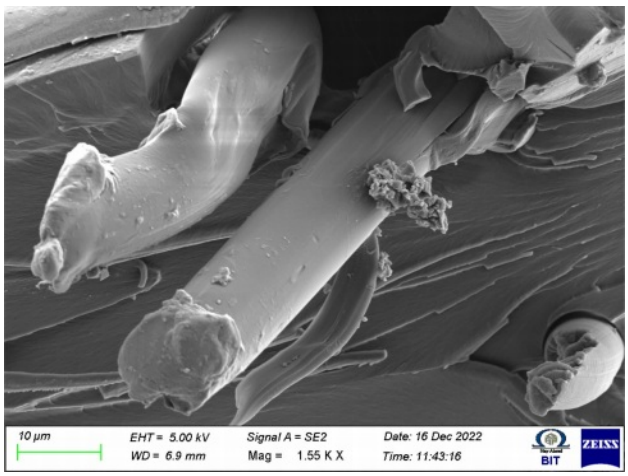

Fig. 1. SEM image of Aramid Fiber Reinforced Polymer composite at failure.

Aramid Fiber-Reinforced Polymer (AFRP) composites significantly impacts their overall properties, encompassing hardness, wear resistance, thermal stability, microstructure, and chemical durability. However, the outcomes of these alterations can vary, offering advantages or challenges depending on the intended application and desired characteristics of the composite. Oxidation and decarburization have been shown to reduce the hardness, abrasion resistance friction, and possibly even the corrosion resistance of Aramid Fiber-Reinforced Polymer (AFRP) composite coatings deposited via the High-Velocity Oxygen Fuel (HVOF) spraying approach. The below image demonstrates the pre-failure elongation of the composite's fiber matrix. As can be seen in the accompanying table, AFRP composite laminates can store the desirable mechanical properties.

The break force represents the maximum force the material can withstand before fracturing or breaking. For the AFRP composites, the break force is measured at 843.4 N. Flexural strength at yield indicates the ability of the material to resist bending or deformation under a specific load. The AFRP composites have a flexural strength at yield of 24.57 N/mm^2. Flexural strength at break represents the maximum bending strength the material can sustain before fracturing. The AFRP composites exhibit a flexural strength at break of 29.195 N/mm^2. The impact load measures the energy absorbed by the material when subjected to an impact or sudden force. In this case, the AFRP composites absorb an impact load of 0.552 Joules. It's important to note that these values provide an overview of the

mechanical properties of the Aramid Fiber Reinforced Polymer composites and are specific to the materials tested.

Exploratory Approach

Once the Reinforced concrete beams had cured for 60 days, they were put through an assortment of tests that included four-point flexural test.

Building of RC beam

The beams under investigation had a rectangular cross-section measuring 100 mm in width and 150 mm in height, with a length of 2000 mm shown in Fig. 2. The beams were reinforced with two 8 mm diameter tension reinforcement bars and two Φ8 compression reinforcement bars. These steel bars were interconnected using 6 mm stirrups placed at a spacing of 150 mm along the length of the beam, as illustrated in Fig. 4(a). The design of all beams adhered to the specifications outlined in the Indian Standard Code of 456-2000. To prevent failure due to splitting bond, a clear concrete cover of 20 mm was provided to the main flexural reinforcement in all the beams. This cover was applied with the intention of maintaining the integrity of the bond between the reinforcement and the surrounding concrete. The beams underwent a curing period of two

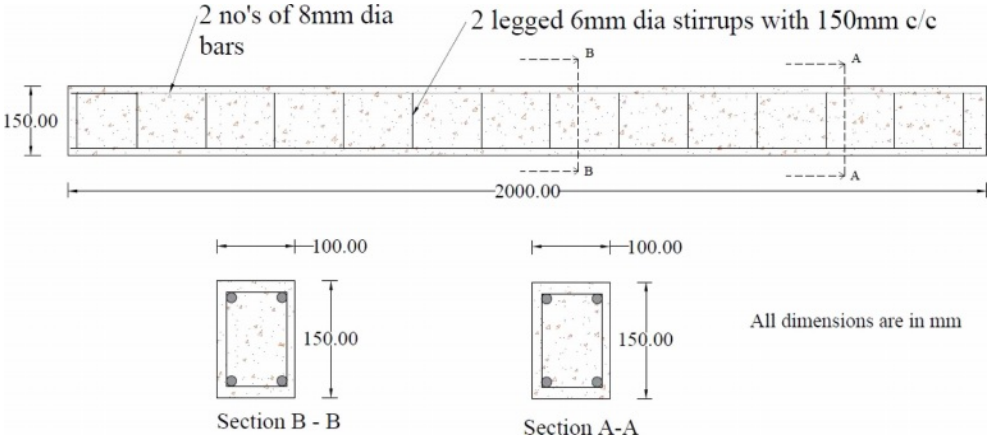

Fig. 2. Reinforced Concrete Beam Cross Sectional Details.

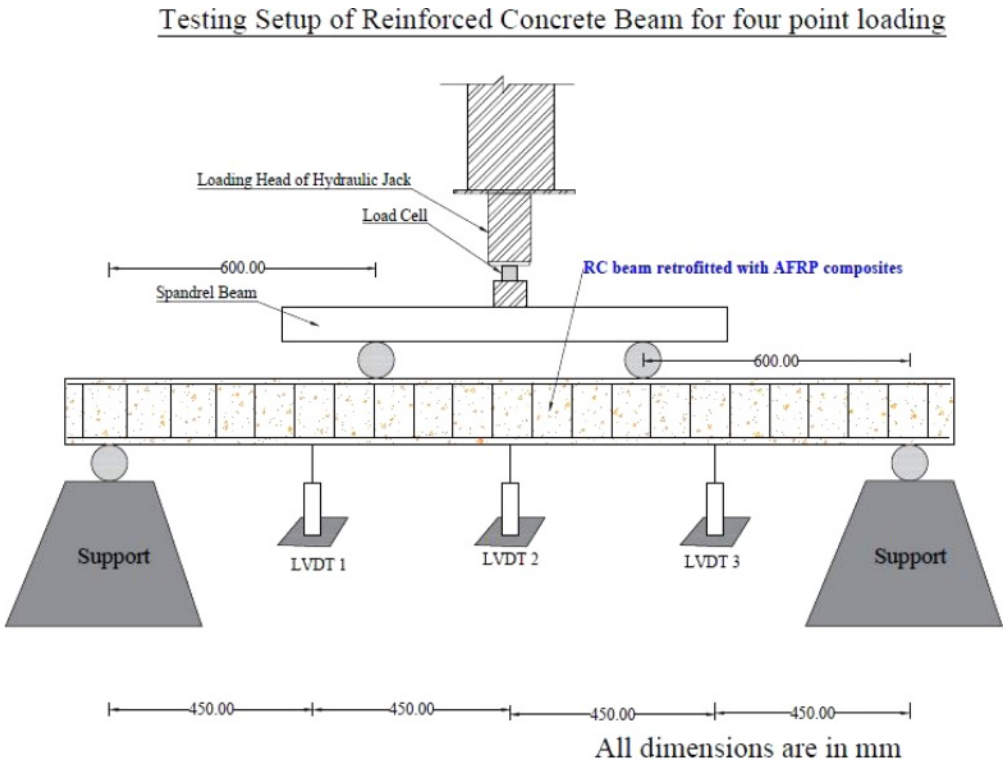

Fig. 3. Experimental test setup for beam.

months before the initial testing phase commenced. This curing process ensured that the concrete achieved adequate strength prior to conducting the experiments.

Control-beam testing

A technique that is referred to as "preloading of RC beam" is one that can be utilised for emulating the amounts of strain and stress that a beam might be subjected to in applications that take place in the real world. Before carrying out the actual test, the beam is put through a procedure in which it is loaded with a predetermined amount of force or load. Before the retrofitting was done, then RC beams being preloaded with load in order to mimic damage [19]. The preloading was carried out utilising the identical set up that was detailed in Fig. 3. Control beam tests revealed that the load necessary to cause cracking in the RC beams was 25.4 kN. The weight is then gradually released in a regulated manner in order to observe any faults that may have occurred while the beam was being tested.

On the beams, four-point bending testing were conducted. This load scenario was chosen due to the fact that it provides a constant maximum moment with no shear in the load-bearing section and a constant maximum shear force between the support and the load. The correlation between the moment and the support and burden was linear. As shown in Fig. 5, the distance between each support was set to 1800 mm, and the burden was distributed in three equal segments along the span. Steel plates were inserted beneath the loads to evenly distribute the weight across the width of the beam. A 1000 kN-capacity crane testing machine was used for the evaluations. Fig. 6 depicts the beam test configuration, and a linearly variable differential transducer (LVDT) was used to measure the displacement at midspan.

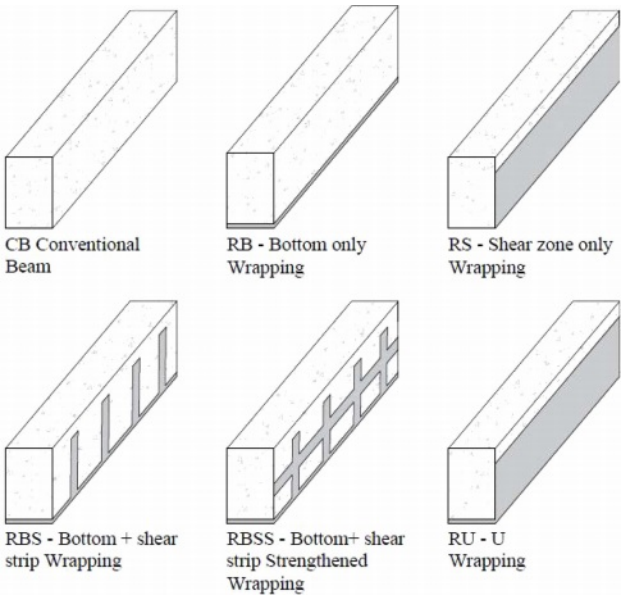

Fig. 4. Peculiar retrofitting layout.

At a load of 20.4 kN, cracks became evident. In the region with constant bending moment, fractures predominated. Fig. 7-a demonstrate the load-displacement graph presenting that yielding occurred at 25.4 kN in member. After the crack spread in the flexural zone, the compression face on the beam experienced a minor crushing of concrete. The maximum force the beam could withstand was measured at 30.6 kN. The failure mode was flexure-based. There was no deboning or shear cracking in the beam.

RC Beams undergoing retrofitting

The RC beams that had been tested were removed from the testing equipment and enhanced with AFRP. Retrofitting of beams was accomplished via wrapping technique with tensile fibre reinforcement in the form of aramid fibre matrix in the polymer composite that produces AFRP laminates. In order to restore the impairment in the researched RC beams, the venule shear and tensile cracks were looked into and epoxy injection was attempted to repair them. For the successful implementation of AFRP strengthening, the preceding procedures are depicted in Fig. 5a-c. At the time of Aramid bonding, the concrete surface is roughened with a wire brush and then washed thoroughly with water to remove all grime. The tested RC beams are left to dry for twenty-four hours.

Now verified RC beams are dust-free, which will improve the adhesion between epoxy and concrete. The AFRP to be utilised in the flexural strengthening was cut into patterns as mention in the Fig. 5c that covers both side faces & the soffit, only bottom tension zone and only side face of the preloaded control beam. To reinforce the beams with AFRP, epoxy, which is created by blending the resin and hardener in the proportions specified by the manufacturer, was prepared. Epoxy adhesive was initially applied with a thickness of 2 mm to a tested RC beam to create a strong bond between the concrete surface and aramid fibre matrix. Aramid fibre matrix for the exposed area of the evaluated RC beam has already been applied to the 2 mm thick epoxy resin-coated concrete surface. Then, discrete epoxy coatings were applied on top of the aramid fibre matrix to create aramid fibre reinforced polymer (AFRP) laminate. Fig. 5(a)-(c) depicts one of the evaluated RC beams retrofitted with AFRP laminates. When the beam was subjected to a small percentage of moment in accordance with their own dead load, AFRP laminates were utilised as a retrofitting element over the member.

Testing of retrofitted beams

Each retrofitted beam underwent testing using the same procedure as the initial load application and it was show in the Fig. 6(a). A four-point flexural

Fig. 5. (a) Application of Epoxy over RC Beam Specimen. (b) Placement of aramid fiber matrix over epoxy coated RC beam specimen. (c) Aramid fiber reinforced RC beam.

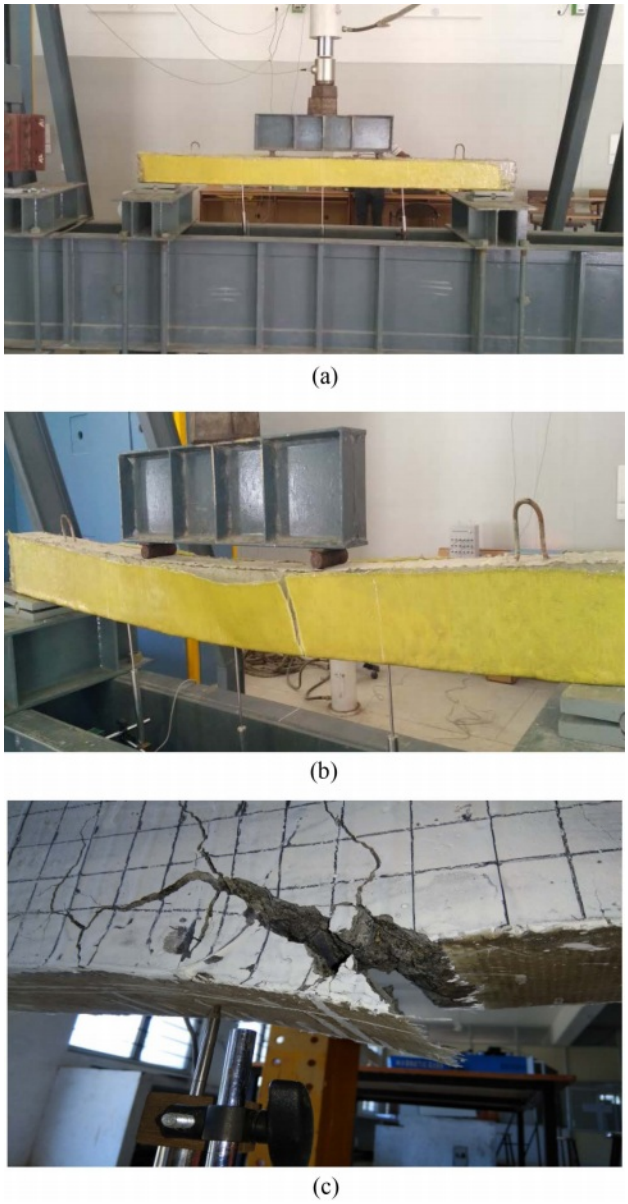

Fig. 6. (a) Testing of U shaped (RU) retrofitted RC beam. (b) Failure of U shaped (RU) retrofitted RC beam. (c) Failure of RC beam retrofitted bottom.

monotonic load was applied to each retrofitted beam, with a span of approximately 1800 mm, as specified in the test setup. The load was applied using a hydraulic jack positioned under a distributing 600 mm distance steel I-beam. An accurately calibrated load cell was used to measure the applied load, ensuring precise measurements. LVDTs (Linear Variable Differential Transformers) were employed to accurately measure the deflection produced during the testing process. Each retrofitted beam was subjected to load until it reached failure. This testing methodology allowed for the examination of the maximum ultimate load carrying capacity of each retrofitted setup.

The experimental testing provided valuable insights into the testing procedure and failure patterns observed in fully retrofitted beams (U shape retrofitting) shown in th Fig. 6(b), bottom-only retrofitted beams (RB) shown in the Fig. 6(c). In the case of RU beams, failure occurred due to tearing at the mid-span when the members reached their ultimate load capacity. For RB beams, debonding of the retrofitted AFRP (Aramid Fiber Reinforced Polymer) laminates was encountered as the beam underwent the ultimate load. This debonding phenomenon compromised the structural integrity of the beam. In the RBS beams, the concrete experienced

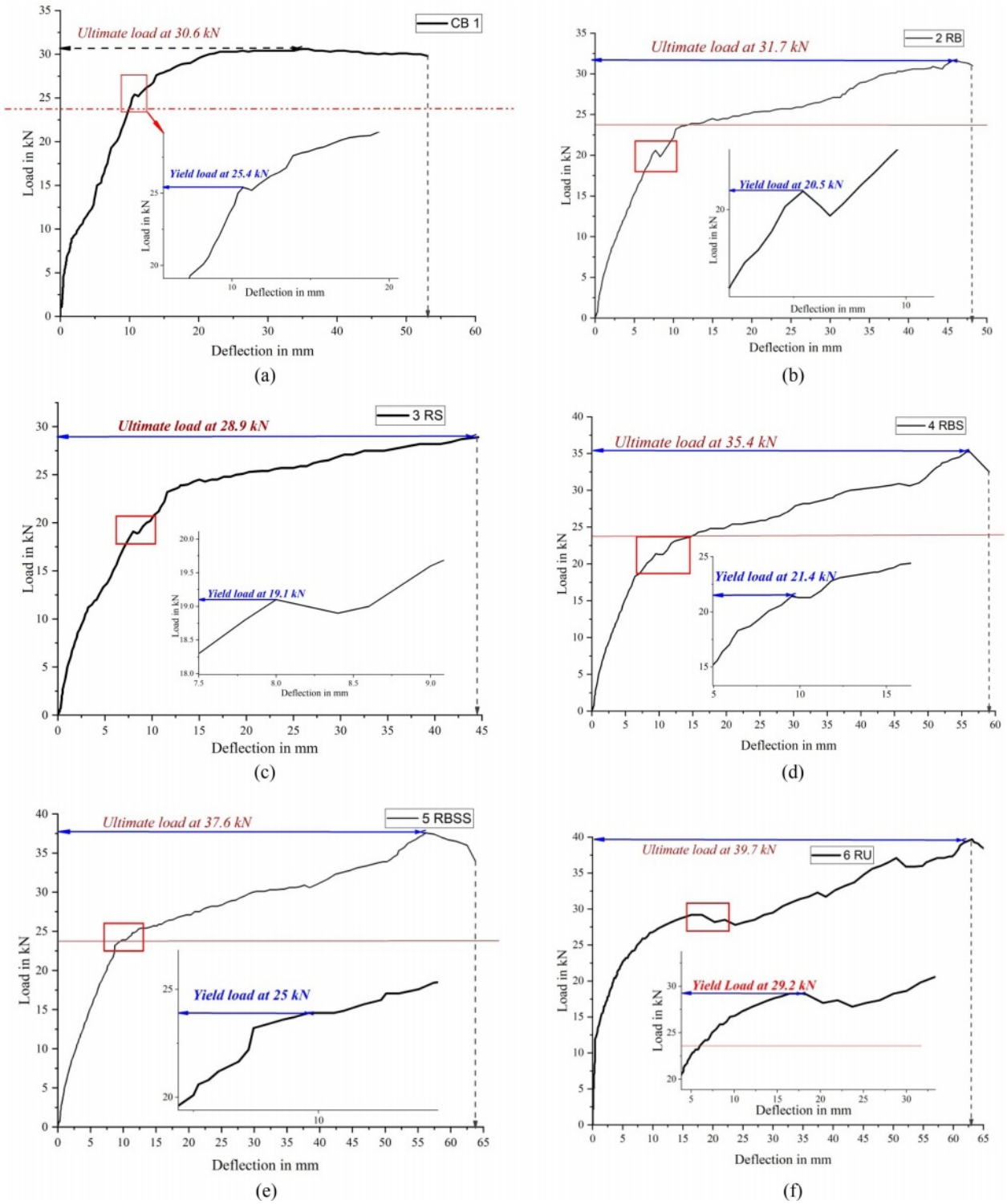

Fig. 7. (a) Load vs Deflection of CB. (b) Load vs Deflection of RB. (c) Load vs Deflection of RS. (d) Load vs Deflection of RBS. (e) Load vs Deflection of RBSS. (f) Load vs Deflection of RU.

crushing failure as the beam reached its ultimate load, resulting in a total collapse of the members. These observations highlight the distinct failure modes associated with each retrofitting technique and provide important information for further analysis and improvement of retrofitting strategies.

Critique of Research Observations

The table below displays the outcomes of an experimental study that compared the effectiveness of various retrofitting patterns on the initially tested RC beam. There were several retrofitting categories discussed,

Table 2. Details of Load-deflection for test specimens.

Beam	Initial Cracking Load in kN	Initial Cracking Deflection in mm	Yield Load in kN	Yield Deflection in mm	Maximum Load in kN	Maximum Deflection in mm	Stiffness
CB	12.5	5	25.40	13.00	30.60	52.00	0.59
RB	11.8	6	20.50	9.00	31.70	45.80	0.69
RS	10.6	4.5	19.20	8.00	28.90	48.00	0.60
RBS	13.8	7.6	21.30	9.50	35.40	56.00	0.63
RBSS	14.6	8.3	25.90	12.00	37.60	56.00	0.67
RU	15.8	9.1	29.20	15.00	39.70	63.00	0.63

including RU, RB, RS, RBS, and RBSS.

Due to the wrapping technique used in retrofitting, the high initial cracking of a CB beam persists even after the beam has been strengthened. The first recorded cracks can be seen as a surface debonding on the AFRP laminates covering the beam. The initial cracking load and deflection of the CB beam were 12.5 kN and 10.6 kN, respectively, whereas those of the RB, RS, RBS, RBSS, and RU beams were 11.8 kN, 13.8 kN, 14.6 kN, and 15.8 kN, respectively. The CB beam, like the others, exhibited the standard 5 mm initial cracking deflection, followed by 6 mm for the RB beam, 4.5 mm for the RS beam, 7.6 mm for the RBS beam, 8.3 mm for the RBSS beam, and 9.1 mm for the RU beam which were shown in the Fig. 7(a)-(f). At a certain load and deflection, beams begin to undergo significant plastic deformation, which is represented by the yield load and deflection. Yield loads for the other beams ranged from 19.2 kN (RS) to 29.2 kN (RU), with 20.5 kN being the lowest for the RB beam. Similarly, the RB beam had the smallest yield deflection of 9 mm, while the RS beam's was 8 mm and the RU beam's was 15 mm. Maximum allowable stress in the beams is represented by the product of the ultimate load and the resulting deflection. With a maximum load of 30.6 kN, the CB beam was followed by the progressively heavier RB, RS, RBS, RBSS, and RU beams. At full load, the highest deflection measured ranged from 45.8 mm (RB) to 63 mm (RU). When AFRP laminates are applied over an existing RC beam, the beam's stiffness increases because of the laminates' high modulus of elasticity. Here the beams' stiffness is indicative of their resistance to deformation when loaded. Higher values of stiffness suggest less deformation because they are inversely proportional to deflection. The remaining beams' stiffness ratings are all between 0.59 (CB) and 0.69 (RB). Utilizing a retrofitting approach that combines reinforcement in both flexural and shear zones, specifically through the application of U-shaped wraps around reinforced concrete beams, leads to a noticeable improvement in their bending capacity, deflection ductility, and energy ductility. Overall, the data indicate that the RB beam was weaker than the others in terms of cracking, yield, and maximum load. Initial cracking load and deflection were greatest for the CB beam, while the RU beam recorded the greatest yield load, maximum load, and deflection. There wasn't much variation in the stiffness values between the beams, with the RB beam being slightly stiffer than the others.

The Table 3 provides valuable insights into the structural properties of various beams, including the area of retrofitting, deflection ductility, and energy ductility. Beginning with the CB beam indicating the absence of any retrofitting intervention. Despite this, the CB beam exhibits a deflection ductility of 4.00, implying its capacity to undergo moderate deformations before structural failure. However, its energy ductility of 1.84 suggests a relatively lower ability to dissipate energy compared to its maximum energy absorption potential. Moving on to the RB beam, it has a

Table 3. Structural parameters of test specimens

Beam Type	Structural Properties of Retrofitted Beam				
	Deflection ductility	Energy upto Yield point	Energy upto Ultimate point	Energy Ductility	Retrofitted beam Area in cm^2
CB	4.00	114.15	210.52	1.84	0
RB	5.09	64.89	342.35	5.28	2000
RS	6.00	62.00	252.19	4.07	6000
RBS	5.89	85.00	548.25	6.45	2600
RBSS	4.67	95.00	577.47	6.08	4600
RU	4.20	94.65	580.23	6.13	8000

retrofitting area of 2000.00 cm² on the bottom face of RC beam. With a deflection ductility of 5.09, the RB beam demonstrates an increased ability to withstand significant deformations before reaching failure. Furthermore, its energy ductility of 5.28 signifies an improved capacity to dissipate energy in relation to its maximum energy absorption potential. The RS beam, with a retrofitting area of 6000.00 cm^2, showcases a remarkable deflection ductility of 6.00. This implies its resilience against substantial deformations before structural failure. However, the energy ductility of the RS beam is recorded as 4.07, suggesting a moderate capacity for energy dissipation compared to its maximum energy absorption potential. The RBS beam exhibits a retrofitting area of 2600.00 cm^2, indicating the extent of the retrofitting measures implemented. With a deflection ductility of 5.89, the RBS beam demonstrates a notable ability to endure significant deformations. Moreover, its energy ductility of 6.45 signifies a high energy dissipation capacity relative to its maximum energy absorption potential. In the case of the RBSS beam, the retrofitting area measures 4600.00 cm^2, indicating a substantial retrofitting intervention. The beam displays a deflection ductility of 4.67, indicating its capability to withstand moderate deformations before failure. Furthermore, its energy ductility of 6.08 highlights a high energy dissipation capacity compared to its maximum energy absorption potential. Lastly, the RU beam exhibits a retrofitting area of 8000.00 cm^2, representing an extensive retrofitting effort. The beam demonstrates a deflection ductility of 4.20, indicating its capacity to withstand moderate deformations. Moreover, its energy ductility of 6.13 signifies a high energy dissipation capability relative to its maximum energy absorption potential. In summary, the table showcases the retrofitting areas of the different beams, as well as their respective deflection ductility and energy ductility. These results provide valuable insights into the structural behaviour and retrofitting performance of the beams, allowing for informed decision-making in the field of structural engineering.

Aramid FRP's contribution to the structural behaviours of retrofitted beams

The inclusion of aramid Fiber Reinforced Polymer (FRP) in the retrofitting process significantly contributes to the structural behaviour of the retrofitted beams which discussed with experimental results in Table 2. Aramid FRP offers several advantageous properties that enhance the performance and strength of the beams. Firstly, aramid FRP provides high tensile strength and stiffness, which improves the overall load-carrying capacity of the retrofitted beams. This reinforcement effectively resists the development and propagation of cracks, preventing or delaying failure mechanisms such as concrete crushing or steel yielding. Additionally, aramid FRP exhibits excellent fatigue resistance, ensuring the retrofitted beams can withstand repeated loading cycles without significant degradation in performance. This property is particularly beneficial in applications where the beams are subjected to dynamic or cyclic loading conditions. Moreover, aramid FRP has a low weight-to-strength ratio, meaning it adds minimal additional weight to the beams while significantly increasing their load-carrying capacity. This characteristic is especially advantageous for retrofitting applications, as it minimizes the additional dead load imposed on the existing structures. Furthermore, aramid FRP possesses exceptional corrosion resistance, making it suitable for retrofitting beams in harsh environmental conditions or in structures exposed to corrosive agents. This corrosion resistance ensures the long-term durability and service life of the retrofitted beams. Overall, the incorporation of aramid FRP in the retrofitting process enhances the structural behaviours of the beams by improving their load-carrying capacity, increasing resistance to cracking and fatigue, reducing additional weight, and providing corrosion protection. These contributions make aramid FRP a valuable material for retrofitting applications, effectively enhancing the performance and longevity of the retrofitted beams.

Different modes of failure exhibited by beam specimens

RC Beams retrofitted with AFRP laminates exhibited different modes of failure, in different retrofitting pattern were observed. Significant debonding mode of failure observed in retrofitted specimens of RS and RBS. Through the experimental results it shows that application of AFRP laminates in shear zone doesn't influence the flexural capacity of members. Debonding failure occurs when the bond between the aramid FRP and the concrete substrate is compromised, leading to reduced load transfer capacity and performance which was evidently shown in energy ductility in Table 2.

Aramid FRP laminate materials possess high tensile strength; however, they can still experience rupture or fiber breakage under extreme loading conditions. RB, RBSS and RU retrofitted beam specimens reported rupture failure during ultimate load.

The percentage of FRP rupture failure in retrofitted beams varies depending on factors such as the type of aramid FRP used and the level of applied loads. Reported failure percentages range from 10% to 30% in studies.

Delamination: Delamination refers to the separation of layers within the aramid FRP laminate. This failure mode is influenced by factors such as adhesive quality, surface preparation, and installation techniques. Reported delamination failure percentages in retrofitted beams range from 5% to 15%.

Concrete Crushing: Retrofitted beams may experience concrete crushing failure, particularly in compression-

dominated loading conditions. The percentage of concrete crushing failure depends on factors such as the compressive strength of the concrete and the level of applied loads. Reported failure percentages range from 10% to 20%.

Shear Failure: Shear failure in retrofitted beams can occur along the interface between the aramid FRP and the concrete, or within the concrete itself. The percentage of shear failure varies depending on factors such as the shear strength of the retrofitting system and the applied loading conditions. Reported failure percentages range from 10% to 25%.

The experimental testing of beams retrofitted with aramid FRP has shown many mechanisms of failure, one of which involves the debonding of aramid FRP composites after the beam has reached its maximum load capacity. Aramid fiber-reinforced polymer (FRP) composites also experience rupture failure in RB-type retrofitting, whereby the retrofitting is applied only to the bottom face. This results in a catastrophic collapse of the retrofitted beam. The failure modes of retrofitted beams may be influenced by several factors, including the kind of aramid fiber-reinforced polymer (AFRP) and the applied load levels. It is observed that the use of epoxy materials in retrofitting might lead to brittle behavior in cases where there is a deficiency in fiber reinforcement. The experimental test specimens were appropriately prepared, and measures were taken to reduce any sharp edges prior to the application of epoxy [21]. It is important to note that the percentages mentioned above are approximate values based on general observations and studies. The actual failure modes and their percentages can vary depending on specific project conditions, material properties, and quality of installation. It is recommended to consult design guidelines and conduct detailed structural analysis to assess the specific failure modes and risks associated with beams retrofitted with aramid FRP in a particular project.

Conclusion

The experimental study comparing the retrofitting patterns of Aramid Fiber Reinforced Polymer (AFRP) composites on RC beams provided valuable insights into their structural behaviors and performance. The results highlighted the effectiveness of different retrofitting techniques and shed light on the contributions of aramid FRP to the enhanced properties of the retrofitted beams.

The comparison of load-deflection characteristics among the different beams revealed variations in cracking load, yield load, maximum load, and stiffness. The CB beam, without any retrofitting intervention, exhibited high initial cracking load but had limitations in terms of maximum load and stiffness. On the other hand, the RU beam, with extensive retrofitting, showed the highest yield load, maximum load, and deflection. The RB beam, however, displayed weaker performance compared to other beams in terms of cracking, yield, and maximum load.

The structural parameters of the retrofitted beams, including deflection ductility and energy ductility, provided insights into their ability to withstand deformations and dissipate energy. The retrofitting areas of the beams varied, with the RS beam showing the largest retrofitting area. The RBSS and RBS beams exhibited higher deflection ductility and energy ductility, indicating their capacity to withstand significant deformations and dissipate energy effectively.

The inclusion of aramid FRP in the retrofitting process contributed to the improved structural behaviors of the beams. Aramid FRP provided high tensile strength, stiffness, fatigue resistance, and corrosion resistance, enhancing the load-carrying capacity, crack resistance, durability, and overall performance of the retrofitted beams. Additionally, aramid FRP's low weight-to-strength ratio minimized the additional dead load on the existing structures.

The modes of failure observed in the retrofitted beams included debonding, rupture, delamination, concrete crushing, and shear failure. The percentages of these failure modes varied depending on factors such as the type of aramid FRP used, applied loads, and installation techniques. It is crucial to consider these failure modes and conduct detailed structural analysis when retrofitting beams with aramid FRP to ensure optimal performance and safety.

Overall, the study demonstrated the effectiveness of AFRP retrofitting in restoring and improving the structural functionality of RC beams. The findings can guide engineers and researchers in selecting appropriate retrofitting patterns and optimizing the design and implementation of aramid FRP composites for structural enhancement.

Practical application

Aramid fiber reinforced polymer (FRP) composites have numerous and far-reaching practical uses, including the retrofitting of RC beams. Engineers and researchers can learn more about the efficacy and adaptability of this technology by analyzing contemporary situations and case studies. The use of Aramid FRP composites in retrofitting puts interesting options to increase the endurance of service and improve the working condition of RC beam structures as society faces standing difficulties linked to deteriorating infrastructure, seismic hazards, and sustainability.

Acknowledgements

This study was done in the Structural Engineering laboratory at Kongu Engineering College in Perundurai, Erode, Tamil Nadu-638060, India.

References

1. S. Ahmad, A.M.A. Sharif, M.A. Al-Osta, M.M. Al-Zahrani, A.M. Sharif, and M.A. Al-Huri, Structures 48 (2022) 1772-1787.
2. S. Ahmed, E.Y. Mohamed, H.A. Mohamed, and M. Emara, Structures 49 (2022) 106-123.
3. E.Z. Beydokhty and H. Shariatmadar, Lat. Am. J. Solids Struct. 13 (2016) 880-896.
4. S. Kothandaraman and G. Vasudevan, Constr. Build. Mater. 24[11] (2010) 2208-2216.
5. K.B. Shima, T. Kishib, C.S. Choic, and T.H. Ahna, J. Ceram. Process. Res. 16 (2015) 1-13.
6. M. Srinivasan, S. Ramesh, S. Sundaram, and R. Viswanathan, J. Ceram. Process. Res. 22[3] (2021) 345-355.
7. G. Peng, D. Niu, X. Hu, S. Zhong, and D. Huang, Eng. Struct. 267 (2022) 114713.
8. K. Sengun and G. Arslan, Structures 40 (2022) 202-212.
9. K.S. Navaneethan, B. Kiruthika Nandhini, S. Anandakumar, and K.P. Jayakrishna, (2021) 261-275.
10. M.A.G. Silva and H. Biscaia, Compos. Struct. 85[2] (2008) 164-174.
11. M. Shivaperumal, R. Thirumalai, S. Kannan, and Y.K.S.S. Rao, J. Ceram. Process. Res. 23[3] (2022) 404-408.
12. S. Velusamy, A. Subbaiyyan, K. Ramasamy, M. Shanmugamoorthi, V. Vellingiri, Y. Chandrasekaran, and V. Murugesan, Materials Today: Proceedings 65 (2022) 549-553.
13. M. Shanmugamoorthy, S. Velusamy, A. Subbaiyyan, R. Yogeswaran, R. Krishnanbabu, and R. Senthilkumar, Materials Today: Proceedings 65 (2022) 920-924.
14. P. Colajanni and S. Pagnotta, Eng. Struct. 266 (2022) 114589.
15. H.S. Kim and Y.S. Shin, Compos. Struct. 93[2] (2011) 802-811.
16. W. Li and C.K.Y. Leung, J. Compos. Constr. 20[3] (2016) 1-14.
17. S.K.M.P. Thiyaneswaran, K. Nirmalkumar, and V. Sampathkumar, J. Environ. Prot. Ecol. 24[3] (2023) 809-819.
18. G.E. Arunkumar, K. Nirmalkumar, P. Loganathan, and V. Sampathkumar, Glob. Nest J. 25[5] (2023) 126-135.
19. Y.T. Obaidat, S. Heyden, O. Dahlblom, G. Abu-Farsakh, and Y. Abdel-Jawad, Constr. Build. Mater. 25[2] (2011) 591-597.
20. S. Sridhar, S. Nandhakumar, M. Nallusamy, and R. Maguteeswaran, J. Ceram. Process. Res. 23[4] 2022 498-502.
21. K.M. Senthilkumar, N. Kathiravan, L. Girisha, and M. Sivaperumal, J. Ceram. Process. Res. 23[4] 541-545.
22. K.V. Boobala Krishnan, K. Nirmalkumar, V. Sampathkumar, and P.C. Murugan, J. Ceram. Process. Res. 24[4] 714-722.